J|A|C|S
ARTICLES

Published on Web 02/11/2010

Electrochemical Responses and Electrocatalysis at Single Au Nanoparticles

Yongxin Li, Jonathan T. Cox, and Bo Zhang*

Department of Chemistry, University of Washington, Seattle, Washington 98195-1700

Received November 5, 2009; E-mail: zhang@chem.washington.edu

Abstract: Steady-state electrochemical responses have been obtained at single Au nanoparticles using Pt nanoelectrodes. A Au single-nanoparticle electrode (SNPE) is constructed by chemically immobilizing a single Au nanoparticle at a SiO_2-encapsulated Pt disk nanoelectrode, which was previously modified by an amine-terminated silane. The Au SNPE has been characterized by transmission electron microscopy, underpotential deposition of Cu, and steady-state cyclic voltammetry. It has been found that the presence of a single Au nanoparticle enhances the electron transfer from the Pt nanoelectrode to the redox molecules, and the voltammetric response at the Au SNPE depends on the size of the Au nanoparticle. The Au SNPE has been utilized to examine the oxygen-reduction reaction in a KOH solution to explore the feasibility of measuring the electrocatalytic activity at a single-nanoparticle level. It has been shown that the electrocatalytic activity of single Au nanoparticles can be directly measured using SNPEs, and the electrocatalytic activity is dependent on the size of the Au nanoparticles. This study can help to understand the structure−function relationship in nanoparticle-based electrocatalysis.

Introduction

Nanomaterials have received intensive research interest in recent decades due to their unique structure-dependent properties and potential applications in numerous fundamental and applied fields.[1,2] For example, nanoparticles have been extensively utilized as catalysts in chemical synthesis,[3] energy conversion,[4,5] and energy storage.[6] An important aspect of nanoparticles is their structure-dependent catalytic activity.[7,8] It has been shown that the electrocatalytic activity of metal nanoparticles is extremely sensitive to their sizes.[9−12] Due to differences in electrochemical activity at different crystal surfaces, the shape of the nanoparticles also greatly alters their functionality. For example, the catalytic activity of Pt single crystals toward oxygen-reduction reaction (ORR) in H_2SO_4 at the {110} surface is significantly greater than that at the {100} and {111} surfaces.[13] There have been numerous research efforts reported to control the shape of metal nanoparticles to obtain optimized activity in electrocatalysis.[14−19] The composition of metal nanoparticles also plays critical roles in their catalytic activity.[20,21]

Most current studies in electrocatalysis rely on the use of ensembles of nanoparticles to understand the structure−function relationship.[22−24] However, only averaged catalytic properties can be obtained from such experiments. In a typical study, metal nanoparticles are immobilized on a supporting electrode to form a nanoparticle-array electrode, and then their electrochemical responses are measured as a function of the particle structure.[10,25−28] The properties of metal nanoparticles can be complicated due to a combination of multiple effects, such as the interparticle spacing,[29] the quality of the self-assembled monolayers (SAMs), and the size distribution of the particles. There are some excellent examples reported to study the size effects of metal nanoparticles in electrocatalysis using the array method. For example, the Crooks group has shown that the catalytic activity of dendrimer-encapsulated Pt nanoclusters increases with increasing size for ORR.[30] The Zou group has measured the electrocatalytic activities

(1) Rosi, N. L.; Mirkin, C. A. *Chem. Rev.* **2005**, *105*, 1547–1562.
(2) Daniel, M. C.; Astruc, D. *Chem. Rev.* **2004**, *104*, 293–346.
(3) Son, S. U.; Jang, Y.; Park, J.; Na, H. B.; Park, H. M.; Yun, H. J.; Lee, J.; Hyeon, T. *J. Am. Chem. Soc.* **2004**, *126*, 5026–5027.
(4) Park, K. W.; Choi, J. H.; Kwon, B. K.; Lee, S. A.; Sung, Y. E.; Ha, H. Y.; Hong, S. A.; Kim, H.; Wieckowski, A. *J. Phys. Chem. B* **2002**, *106*, 1869–1877.
(5) Gratzel, M. *J. Photochem. Photobiol., A* **2004**, *164*, 3–14.
(6) Wang, Y.; Lee, J. Y.; Deivaraj, T. C. *J. Electrochem. Soc.* **2004**, *151*, A1804–A1809.
(7) Bell, A. T. *Science* **2003**, *299*, 1688–1691.
(8) Somorijai, G. A.; Contreras, A. M.; Montano, M.; Rioux, R. M. *Proc. Natl. Acad. Sci. U.S.A.* **2006**, *103*, 10577–10583.
(9) Haruta, A. *Chem. Rec.* **2003**, *3*, 75–87.
(10) Ye, H.; Crooks, R. M. *J. Am. Chem. Soc.* **2005**, *127*, 4930–4934.
(11) Maillard, F.; Savinova, E. R.; Stimming, U. *J. Electroanal. Chem.* **2007**, *599*, 221–232.
(12) Chen, W.; Kim, J.; Sun, S. H.; Chen, S. W. *Langmuir* **2007**, *23*, 11303–11310.
(13) Markovic, N. M.; Schmidt, T. J.; Stamenkovic, V.; Ross, P. N. *Fuel Cells* **2001**, *1*, 105–116.
(14) Ahmadi, T. S.; Wang, Z. L.; Green, T. C.; Henglein, A.; El-Sayed, M. A. *Science* **1996**, *272*, 1924–1925.
(15) Petroski, J. M.; Green, T. C.; El-Sayed, M. A. *J. Phys. Chem. A* **2001**, *105*, 5542–5547.
(16) Petroski, J. M.; Wang, Z. L.; Green, T. C.; El-Sayed, M. A. *J. Phys. Chem. B* **1998**, *102*, 3316–3320.
(17) Inaba, M.; Ando, M.; Hatanaka, A.; Nomoto, A.; Matsuzawa, K.; Tasaka, A.; Kinumoto, T.; Iriyama, Y.; Ogumi, Z. *Electrochim. Acta* **2006**, *52*, 1632–1638.
(18) Hernandez, J.; Solla-Gullon, J.; Herrero, E.; Aldaz, A.; Feliu, J. M. *J. Phys. Chem. C* **2007**, *111*, 14078–14083.
(19) Solla-Gullon, J.; Vidal-Iglesias, F. J.; Lopez-Cudero, A.; Garnier, E.; Feliu, J. M.; Aldaz, A. *Phys. Chem. Chem. Phys.* **2008**, *10*, 3689–3698.
(20) Stamenkovic, V. R.; Mun, B. S.; Arenz, M.; Mayrhofer, J. J. J.; Lucas, C. A.; Wang, G. F.; Ross, P. N.; Markovic, N. M. *Nat. Mater.* **2007**, *6*, 241–247.
(21) Somorjai, G. A.; Park, J. Y. *Top. Catal.* **2008**, *49*, 126–135.

at bare Au nanoparticles and found that the catalytic activity of Au nanoparticles for the oxidation of CO reaches an optimized value when they are about 4 nm.[29]

Only a few attempts have been reported to directly measure the faradic responses at individual nanoparticles. Bard et al. recently reported an innovative method to measure the diffusion-limited faradic current at single Pt nanoparticles.[31−33] In their experiments, an inert ultramicroelectrode (carbon or gold) was held at a potential where there is no apparent electrochemical reaction occurring. However, when a collision between a Pt nanoparticle and the ultramicroelectrode happens, electrochemical reactions can be detected at the Pt surfaces. Chen's group recently reported a method of measuring the electrocatalytic activity at individual metal nanoparticles and single carbon nanotubes by single-molecule fluorescence.[34] A challenge in utilizing the above methods to correlate the structure−function relationship is the subsequent structural characterization of the same metal nanoparticles with high-resolution electron microscopy. Meanwhile, it could also be difficult to obtain an entire current−voltage response at individual nanoparticles using these methods.

It has become increasingly important to understand the relationship between the functionality of nanoparticles and their structure to more fully utilize the unique catalytic properties of nanoparticles. However, it remains practically difficult to attribute the catalytic activity to the structure of the nanoparticles. To precisely correlate the structure and function of nanoparticle catalysts, both electrochemical responses and high-resolution structural characterizations are needed at a single-nanoparticle level. Nanoelectrodes could provide a particularly useful avenue for this purpose due to their extremely small size. Chen and Kucernak have recently reported the study of ORR at single Pt nanoparticles electrodeposited on carbon nanoelectrodes.[35] Their results show that, using single Pt nanoparticles between ~50 nm and 5 μm, the effect of an ultrahigh mass-transfer rate on the ORR can be readily studied. Interestingly, they have shown that the ORR pathway can be alternated from the regular direct reduction of oxygen (four-electron pathway) toward indirect reduction (two-electron pathway) when the particle size decreases from >5 μm to ~50 nm due to higher mass-transfer rates of H_2O_2 at smaller particles.

Using Pt nanoelectrodes as small as 2 nm in radii,[36] our group has recently studied the electrochemical responses and electrocatalytic activity at single Au nanoparticles. A Au single-nanoparticle electrode (SNPE) has been developed for these studies by immobilizing a single Au nanoparticle at the surface of a nanoelectrode. Figure 1 shows a schematic diagram of an SNPE, in which a single Au nanoparticle is immobilized on a Pt nanodisk. Between the Au nanoparticle and the Pt surface are the silane linker molecules. Single Au nanoparticles in the range of 10−30 nm in diameter have been chemically assembled at the end of a Pt nanoelectrode using (3-aminopropyl)trimethoxysilane (APTMS) as the linker molecule. These novel nanoelectrodes have been characterized using transmission electron microscopy (TEM), underpotential deposition (UPD), and steady-state voltammetry. ORR has been examined at single Au nanoparticles using SNPEs. The steady-state voltammetric responses and the electrocatalysis results show that the electron-transfer kinetics at Au SNPEs is rapid and that the Au SNPEs are excellent nanoprobes for studying electrocatalysis at a single-nanoparticle level. This research not only provides a new electrochemical platform for investigating electrocatalytic nanomaterials, but also suggests a new electroanalytical nanoprobe for many other research areas. For example, SNPEs could be particularly useful in studying electron-transfer kinetics between the nanoelectrode and the metal nanoparticles, therefore providing valuable information for molecular electronics and single-nanoparticle electrochemical sensors.

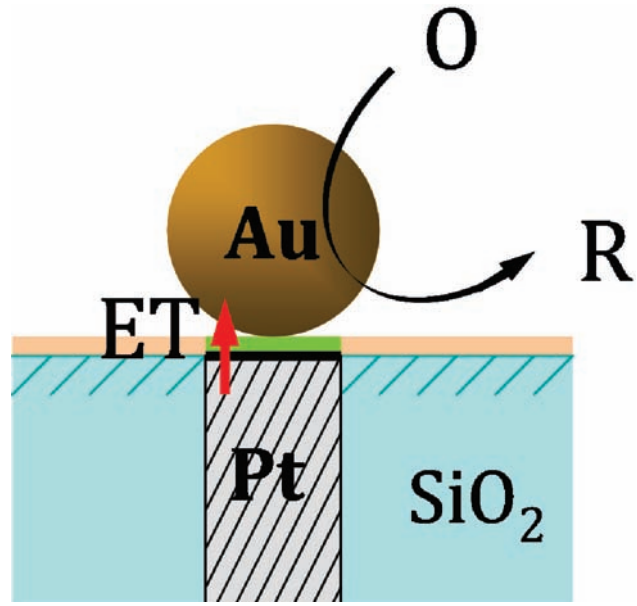

Figure 1. Schematic drawing of a Au SNPE. ET is the abbreviation of electron transfer.

Experimental Section

Chemicals. Potassium ferricyanide ($K_3Fe(CN)_6$; Acros Organics), hexaammineruthenium(III) chloride ($Ru(NH_3)_6Cl_3$; Aldrich), potassium chloride (KCl; Mallinckrodt Baker), APTMS ($(CH_3O)_3Si(CH_2)_3NH_2$; Gelest Inc.), (3-cyanopropyl)dimethylchlorosilane ($Cl(Me)_2Si(CH_2)_3CN$; Fluka), and gold(III) chloride ($HAuCl_4 \cdot 3H_2O$; Aldrich) were of reagent grade quality or better and were used without further purification. All aqueous solutions were prepared from >18 MΩ·cm deionized water obtained from a Barnstead Nanopure water purification system.

Pt Nanoelectrode Fabrication. The Pt nanoelectrodes were fabricated using a laser-assisted pulling method,[36] which involved a four-step process as previously described.[37,38] Briefly, an ultrasharp Pt nanowire tip (<10 nm) was first pulled from a Pt microwire using a laser puller (P-2000, Sutter). A Pt microwire

(22) Crooks, R. M.; Zhao, M.; Sun, L.; Chechik, V.; Yeung, L. K. *Acc. Chem. Res.* **2001**, *34*, 181–190.
(23) Chen, M.; Goodman, D. W. *Acc. Chem. Res.* **2006**, *39*, 739–746.
(24) Burda, C.; Chen, X.; Narayanan, R.; El-Sayed, M. A. *Chem. Rev.* **2005**, *105*, 1025–1102.
(25) Lim, B.; Jiang, M.; Camargo, P. H. C.; Cho, E. C.; Tao, J.; Lu, X.; Zhu, Y.; Xia, Y. N. *Science* **2009**, *324*, 1302–1305.
(26) Ye, H.; Crooks, J. A.; Crooks, R. M. *Langmuir* **2007**, *23*, 11901–11906.
(27) Wang, C.; Daimon, H.; Lee, Y.; Kim, J.; Sun, S. *J. Am. Chem. Soc.* **2007**, *129*, 6974–6975.
(28) Cheng, W.; Dong, S.; Wang, E. *Langmuir* **2002**, *18*, 9947–9952.
(29) Kumar, S.; Zou, S. Z. *Langmuir* **2009**, *25*, 574–581.
(30) Ye, H. C.; Crooks, R. M. *J. Am. Chem. Soc.* **2007**, *129*, 3627–3633.
(31) Xiao, X.; Bard, A. J. *J. Am. Chem. Soc.* **2007**, *129*, 9610–9612.
(32) Xiao, X.; Fan, F.-R. F.; Zhou, J.; Bard, A. J. *J. Am. Chem. Soc.* **2008**, *130*, 16669–16677.
(33) Xiao, X.; Pan, S.; Jang, J. S.; Fan, F.-R. F.; Bard, A. J. *J. Phys. Chem. C* **2009**, *113*, 14978–14982.
(34) Xu, W.; Shen, H.; Kim, Y. J.; Zhou, X.; Liu, G.; Park, J.; Chen, P. *Nano Lett.* **2009**, *9*, 3968–3973.
(35) Chen, S.; Kucernak, A. *J. Phys. Chem. B* **2004**, *108*, 3262–3276.
(36) Li, Y.; Bergman, D.; Zhang, B. *Anal. Chem.* **2009**, *81*, 5496–5502.

Scheme 1. Scheme for the Fabrication of the Au SNPE

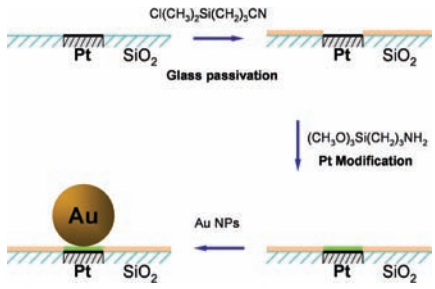

between 5 and 25 μm was prepared by electrochemically etching a 25 μm Pt wire (Alfa Aesar) in a 6 M NaCN solution containing 0.1 M NaOH. The Pt nanowire tip was visualized using a 400× magnification microscope (Olympus, BX51).

The Pt nanowire tip was exposed to make a Pt disk nanoelectrode by a special sealing/polishing process. The pulled Pt nanowire tip was sealed into a borosilicate glass tube (2 mm o.d., Sutter) under in-house vacuum using a hydrogen flame. To expose the Pt nanowire tip, the sealed end was polished using regular sandpaper and alumina suspension on a polishing cloth. The whole process was monitored by using an optical microscope and a homemade ultrasensitive continuity tester to ensure the polishing stops when the very end of Pt is exposed.[39] The size of the Pt nanoelectrode can be calculated from the diffusion-limited steady-state current obtained in a redox solution.[36,40]

Preparation and Characterization of Gold Nanoparticles. Au nanoparticles in the range of 10−30 nm in diameter were prepared by the reduction of $HAuCl_4$ with sodium citrate.[41,42] All glassware was thoroughly cleaned with a fresh piranha solution (1:3 H_2O_2/H_2SO_4) (*caution: piranha solution reacts violently with organic materials; all procedures must be carried out in a ventilation hood with proper eye and hand protection*) and rinsed thoroughly with water before use. In a typical synthesis of ∼14 nm Au nanoparticles, 50 mL of $HAuCl_4$ solution (0.01%, m/v) was brought to a vigorous boil with stirring in a round-bottom flask fitted with a reflux condenser, and 1.8 mL of sodium citrate solution (1%, m/v) was then rapidly added to the flask. The heating and stirring were continued for 15 min, and then the solution was allowed to cool to room temperature with continuous stirring and stored at 4 °C until use. Larger nanoparticles were prepared by reducing the molar ratio of sodium citrate to $HAuCl_4$ in the synthesis. The average sizes of the nanoparticles were determined from TEM characterizations (Supporting Information).

Fabrication of Au SNPEs. The general strategy for the fabrication of Au SNPEs is depicted in Scheme 1. Starting from a Pt disk nanoelectrode, the silanization of the silica surfaces with $Cl(Me)_2Si(CH_2)_3CN$ was described by Wang et al.[43] Following the exposure of the Pt nanodisk, the electrode was rinsed completely in H_2O, EtOH, CH_3CN, and H_2O and then soaked in 1.0 M HNO_3 for 10 min. The electrode was rinsed with H_2O and CH_3CN and then immersed overnight in a CH_3CN solution containing ∼2% (v/v) $Cl(Me)_2Si(CH_2)_3CN$. After that, the electrode was rinsed with CH_3CN and H_2O again.

The modification of the Pt nanodisk with silane was carried out according to previous methods provided by Murray et al.[44−46] with slight modifications. The Pt nanoelectrode from the previous step was cleaned by rinsing with ethanol and water. A layer of Pt oxide was generated by applying a potential of 1.20 V vs Ag/AgCl in 0.5 M H_2SO_4 until the oxidation current decayed to zero, whereupon the electrode was removed from the H_2SO_4 solution while still under potential control (1.20 V), rinsed thoroughly with water, and dried at ca. 50 °C for 30−60 min. The oxidized Pt (PtO) nanoelectrode was placed in an anhydrous toluene solution containing ca. 5% $(CH_3O)_3Si(CH_2)_3NH_2$ for ∼30 min under N_2 protection. The silanized PtO surface was then rinsed thoroughly with toluene, CH_3CN, and water.

In the last step, the silane-modified Pt nanoelectrode was immersed into a solution of Au nanoparticles (as-prepared from previous synthesis) overnight at room temperature, and then was rinsed well with water and subjected to electrochemical measurements.

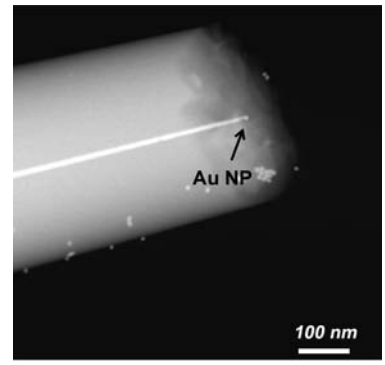

Figure 2. TEM image of a single Au nanoparticle immobilized on a Pt nanoelectrode.

Electrochemical Measurements. A Chem-Clamp voltammeter−amperometer (Dagan) was used as the potentiostat in all electrochemical measurements. The potentiostat was interfaced to a Dell PC through a PCI-6521 data acquisition board (National Instruments) via a BNC-2090 analog breakout accessory (National Instruments). Voltammetric data were recorded using in-house virtual instrumentation written in LabView 8.5 (National Instruments). A one-compartment, two-electrode cell was employed with the cell and preamplifier in a home-built Faraday cage. A Ag/AgCl electrode (Bioanalytical Sciences, Inc.) was used as the reference electrode.

Transmission Electron Microscopy. TEM images of Au nanoparticles, SiO_2-coated Pt nanoelectrodes, and Au SNPEs were acquired on a Tecnai G2 F20 (FEI) microscope. The imaging of the Au nanoparticles was carried out on a carbon film (Ted-Pella). Pt nanoelectrodes and Au SNPEs were mounted on a Cu grid (SPI) using Ag paint (SPI) before TEM imaging. No additional coatings were performed prior to imaging of the nanoelectrodes or SNPEs.

Results and Discussion

TEM Characterization of Au SNPEs. One of the challenges in correlating the catalytic function to the structural characteristics of nanoparticles is the direct high-resolution imaging of single nanoparticles. TEM is one of most popular methods to provide atomic resolution structural information of nanoparticles.[47] The application of ultrasmall Pt nanoelectrodes has made it possible to directly characterize single Au nanoparticles with TEM. Figure 2 shows an example of a TEM image of a

(37) Shao, Y.; Mirkin, M. V.; Fish, G.; Kokotov, S.; Palanker, D.; Lewis, A. *Anal. Chem.* **1997**, *69*, 1627–1634.
(38) Katemann, B. B.; Schuhmann, W. *Electroanal.* **2002**, *14*, 22–28.
(39) Zhang, B.; Galusha, J.; Shiozawa, P. G.; Wang, G.; Bergren, A. J.; Jones, R. M.; White, R. J.; Ervin, E. N.; Cauley, C. C.; White, H. S. *Anal. Chem.* **2007**, *79*, 4778–4787.
(40) Saito, Y. *Rev. Polarogr.* **1968**, *15*, 177–187.
(41) Frens, G. *Nature* **1973**, *241*, 20–22.
(42) Nath, N.; Chilkoti, A. *Anal. Chem.* **2004**, *76*, 5370–5378.
(43) Wang, G.; Zhang, B.; Wayment, J. R.; Harris, J. M.; White, H. S. *J. Am. Chem. Soc.* **2006**, *128*, 7679–7686.
(44) Murray, R. W. *Acc. Chem. Res.* **1980**, *13*, 135–141.
(45) Lenhard, J. R.; Murray, R. W. *J. Electroanal. Chem.* **1977**, *78*, 195–201.
(46) Chen, C. H.; Hutchison, J. E.; Postlethwaite, T. A.; Richardson, J. N.; Murray, R. W. *Langmuir* **1994**, *10*, 3332–3337.
(47) Wang, Z. L.; Gao, R. P.; Nikoobakht, B.; El-Sayed, M. A. *J. Phys. Chem. B* **2000**, *104*, 5417–5420.

single Au nanoparticle immobilized on a Pt nanoelectrode. It can be seen from the TEM image that a single Au nanoparticle is attached on the Pt disk. The immobilization is mainly due to the electrostatic interaction between the Au nanoparticle and the amino-terminated surface.[48,49] The Pt nanodisk has been measured to be ~10 nm, while the Au nanoparticle is ~15 nm in diameter. Some other Au nanoparticles can also be found on the SiO_2 surfaces far away from the Pt disk possibly due to physical adsorption. The ability of directly imaging single nanoparticles chemically attached at a nanoelectrode is important for the correlation of the structure of the nanoparticle with its functionality.

The Pt nanoelectrode used in Figure 2 was prepared by polishing the Pt nanotip directly on a polishing surface.[50] In our polishing procedure, due to bending of the Pt tip upon contacting the polishing surface and/or mechanical vibration, most of the Pt nanoelectrodes show discontinuity in the Pt nanowires. Therefore, we should point out that we had a low success rate (<5%) in preparing useful ultrasharp Pt nanoelectrodes for TEM imaging. To obtain TEM images at even higher resolutions, a smaller tip dimension is preferred. We believe that these smaller ultrasharp Pt nanoelectrodes can be prepared by focused ion-beam (FIB) milling.[51]

UPD of Cu at Au SNPEs. UPD of Cu has been carried out at Au SNPEs to estimate the size of the nanoparticle electrodes. UPD has been widely applied to measure the areas of various electrodes.[52] A monolayer of adatoms is formed in the UPD process, which allows for an easy calculation of the electrode area based on the charge needed to strip the adatoms. Ag,[53] Pb,[54] and Cu[55,56] are often utilized in UPD at various electrode surfaces. Very recently, Mirkin's group reported the characterization of nanometer-sized Pt electrodes using Cu UPD.[57]

To estimate the geometric area of a single Au nanoparticle immobilized at the Pt nanoelectrode, a monolayer of Cu adatoms has been first deposited at the Au SNPE.[58,59] Before stripping, the Au SNPE was held in a 10 mM $CuSO_4$ solution at 0 V (vs Ag/AgCl) for a time period between 10 s and 5 min. Then the electrode was scanned at 100 mV/s from 0 to 0.6 V (vs Ag/AgCl) to oxidize the Cu adatoms. Figure 3a shows a series of voltammetric responses of a Au SNPE after UPD of Cu for different time durations. The amount of charge for the oxidation of Cu has been integrated for each case in Figure 3a. Figure 3b shows the amount of charge plotted as a function of the holding time. One can see that the Cu deposition at the Au SNPE takes

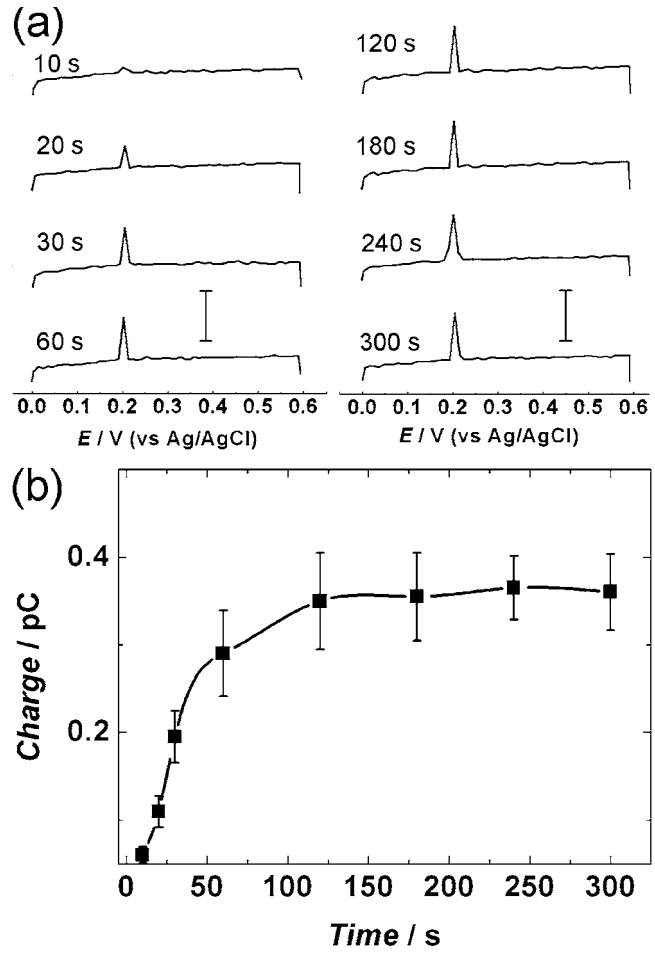

Figure 3. (a) Voltammetric responses of underpotential deposited copper from a 24 nm Au SNPE (Pt electrode diameter ~10 nm, scan rate 100 mV/s). Before stripping, the electrode was held at 0 V vs Ag/AgCl for 10 s, 20 s, 30 s, 1 min, 2 min, 3 min, 4 min, and 5 min. (b) Relationship between the charge obtained from each stripping peak and the UPD holding time. The scale bars in (a) are 3 pA.

~120 s to saturate the Au surfaces. The surface area of the Au nanoparticle was estimated on the basis of the number of Cu adatoms needed to saturate the Au surface. A 410 $\mu C/cm^2$ conversion factor was used to calculate the surface area of the SNPE.[57] From Figure 3, the radius of the Au nanoparticle has been determined to be ~84 nm, which is ~7 times larger than the average radii of the Au colloids (12 nm). The corresponding roughness factor (~50) suggests that Cu UPD, most likely, took place on the lateral surface of the Pt wire.[57] A very long saturation time (~2 min) required for Cu UPD indeed supports this conclusion.

Voltammetric Responses of Au SNPEs in H_2SO_4. The presence of a single Au nanoparticle at the Pt nanodisk electrode can be indicated by continuous sweeping in a 0.5 M H_2SO_4 solution. Figure 4a displays the voltammetric responses of a 24 nm Au SNPE in a 0.5 M H_2SO_4 solution. One can notice the major differences between the initial scans and the subsequent scans in Figure 4a. Initially, the voltammetric response shows a cathodic peak around +0.67 V and an anodic peak around +1.12 V, which we believe correspond to the reduction of gold oxide to Au and the subsequent oxidation of Au,[60] respectively, indicating the presence of

(48) Grabar, K. C.; Smith, P. C.; Musick, M. D.; Davis, J. A.; Walter, D. G.; Jackson, M. A.; Guthrie, A. P.; Natan, M. J. *J. Am. Chem. Soc.* **1996**, *118*, 1148–1153.
(49) Zhu, T.; Fu, X.; Mu, T.; Wang, J.; Liu, Z. *Langmuir* **1999**, *15*, 5197–5199.
(50) Sun, P.; Mirkin, M. V. *Anal. Chem.* **2006**, *78*, 6526–6534.
(51) Lanyon, Y. H.; Marzi, G. D.; Watson, Y. E.; Quinn, A. J.; Gleeson, J. P.; Redmond, G.; Arrigan, D. W. M. *Anal. Chem.* **2007**, *79*, 3048–3055.
(52) Kolb, D. M.; Przasnys, M.; Gerische, H. *J. Electroanal. Chem.* **1974**, *54*, 25–38.
(53) Tindall, G. W.; Bruckens, S. *Electrochim. Acta* **1971**, *16*, 245–246.
(54) Adzic, R.; Yeager, E.; Cahan, B. D. *J. Electrochem. Soc.* **1974**, *121*, 474–484.
(55) Tindall, G. W.; Cadle, S. H.; Bruckenstein, S. *J. Am. Chem. Soc.* **1969**, *91*, 2119–2120.
(56) Cadle, S. H.; Bruckenstein, S. *Anal. Chem.* **1971**, *43*, 932–933.
(57) Zhan, D.; Velmurugan, J.; Mirkin, M. V. *J. Am. Chem. Soc.* **2009**, *131*, 14756–14760.
(58) Arrigan, D. W. M.; Iqbal, T.; Pickup, M. J. *Electroanalysis* **2001**, *13*, 751–754.
(59) Nakamura, M.; Endo, O.; Ohta, T.; Ito, M.; Yoda, Y. *Surf. Sci.* **2002**, *514*, 227–233.
(60) Cadle, S. H.; Bruckenstein, S. *Anal. Chem.* **1974**, *46*, 16–20.

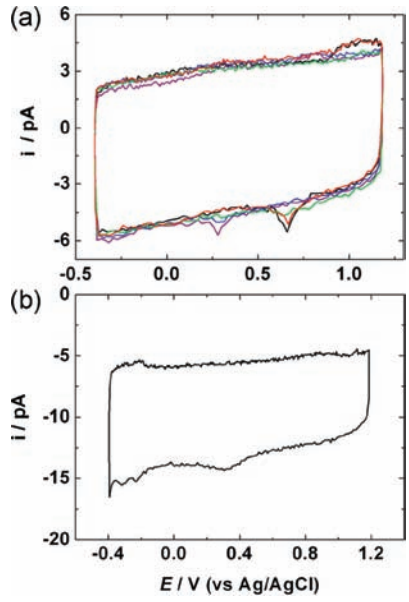

Figure 4. (a) Voltammetric responses of a 24 nm Au SNPE in a 0.5 M H_2SO_4 solution after 1st time scanning (black), 10th time scanning (red), 50th time scanning (green), 200th time scanning (blue), and 500th time scanning (purple) (scan rate 100 mV/s). (b) Voltammetric response of a bare Pt disk nanoelectrode in a 0.5 M H_2SO_4 solution (electrode radius ~10 nm, scan rate 100 mV/s).

Au at the nanoelectrode. The cathodic peak potential for Au is slightly lower than previously reported (~0.8 V vs Ag/AgCl), which may possibly be due to the small size of the Au nanoparticle. In fact, Ivanova and Zamborini have recently reported that the oxidation potential for Ag nanoparticles shifts negatively as the nanoparticle size decreases.[61] In the following cycles, the above anodic and cathodic peaks were observed to decrease gradually and eventually disappear after ~200 cycles of scanning (the blue curve), which could be due to the dissolution of Au after continuous sweeping.[60] However, one should also notice the appearance of a new cathodic peak (the green curve) at 0.28 V vs Ag/AgCl, which gradually increased with increasing sweep numbers (purple curve). We believe this new cathodic peak is originated from the reduction of platinum oxide at the Pt surface,[62−64] indicating the possible reappearance of Pt after removal of the Au and the silane layer by sweeping. The cathodic peak located at around 0.28 V vs Ag/AgCl in Figure 4a is also lower than the cathodic potential previously reported for Pt in H_2SO_4. The reason may be the small size of the Pt electrode. In fact, the cyclic voltammogram of a bare Pt nanoelectrode (radius ~10 nm) in H_2SO_4 is given in Figure 4b. It can be seen that the cathodic peak position is extremely similar to the cathodic peak position in Figure 4a. The size of the Au nanoparticle at the SNPE has been estimated to be ~38 nm in diameter, calculated from the number of Au atoms from the cathodic peak at 0.67 V in Figure 4a, which is larger than the average diameter (24 nm) of the Au nanoparticles used in preparing the electrode. However, this result does indicate the presence of both Au and Pt at the Au SNPEs.

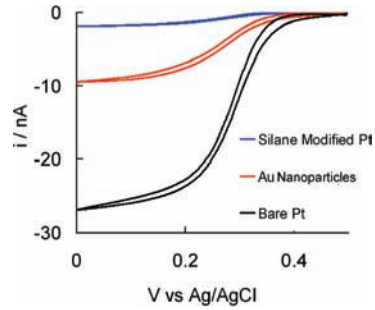

Figure 5. Voltammetric responses of a 25 μm Pt microelectrode in a 5.0 mM $K_3Fe(CN)_6$ solution containing 0.2 M KCl before modification (black), after modification with APTMS (blue), and after modification with 14 nm Au nanoparticles (red) (scan rate 10 mV/s).

Steady-State Voltammetric Response at Au Nanoparticle Arrays on a Pt Microelectrode. Figure 5 displays the voltammetric responses at 10 mV/s of a 25 μm Pt microelectrode before modification (black), after modification with APTMS (blue), and after modification with 14 nm Au nanoparticles (red). The diffusion-limited steady-state current at the Pt microelectrode has been reduced significantly after modification with APTMS due to the blocking of the electron transfer by the silane layer. However, when the Au nanoparticles are assembled at the modified Pt electrode, the steady-state limiting current is greatly increased. One should notice that the steady-state current at the Au nanoparticle array is only 30% of the total current observed at the bare Pt electrode possibly due to a relatively low density of coverage. It has been reported that increasing the particle density can increase the peak current at an array of Au nanoparticles assembled on a macroscopic electrode.[65] However, the peak current obtained at the bare electrode should represent the maximum possible current on nanoparticle arrays on the same electrode. In the case of a single Au nanoelectrode, however, the diffusion-limited steady-state current can actually exceed that obtained at the bare nanoelectrode, as shown in the following experiments.

Steady-State Voltammetric Response at Au SNPEs. The Au SNPEs have been examined using steady-state cyclic voltammetry. Figures 6 and 7 show a comparison of the steady-state voltammetric responses of Au SNPEs, APTMS-modified Pt nanoelectrodes, and bare Pt nanodisks in aqueous solutions containing 5 mM $Fe(CN)_6^{3-}$ (Figure 6) and 5 mM $Ru(NH_3)_6^{3+}$ (Figure 7). From Figure 6a, for example, it can be seen that a typical sigmoidal shaped voltammetric response was observed using an 8 nm bare Pt disk nanoelectrode (black). After modification with APTMS at the Pt, the steady-state limiting current was greatly reduced (red), indicating the blockage of electron transfer due to the silane modification. However, when a 14 nm Au nanoparticle was immobilized at the surface of the Pt, the limiting current was greatly enhanced (green). Similar enhancements have been previously reported using an array of Au nanoparticles at macroscopic electrodes.[66−68] It is interesting to note that the inhibition of the voltammetric current for the nanoelectrode is different from that for 25 μm electrodes. For

(61) Ivanova, O. S.; Zamborini, F. P. *J. Am. Chem. Soc.* **2010**, *132*, 70–72.
(62) Facci, J.; Murray, R. W. *J. Electroanal. Chem.* **1980**, *112*, 221–229.
(63) Biegler, T.; Rand, D. A. J.; Woods, R. *J. Electroanal. Chem.* **1971**, *29*, 269–277.
(64) Attard, G. S.; Bartlett, P. N.; Coleman, N. R. B.; Elliott, J. M.; Owen, J. R.; Wang, J. H. *Science* **1997**, *278*, 838–840.
(65) Diao, P.; Guo, M.; Zhang, Q. *J. Phys. Chem. C* **2008**, *112*, 7036–7046.
(66) Brown, K. R.; Fox, A. P.; Natan, M. J. *J. Am. Chem. Soc.* **1996**, *118*, 1154–1157.
(67) Shipway, A. N.; Katz, E.; Willner, I. *ChemPhysChem* **2000**, *1*, 18–52.
(68) Zhang, B.; Zhang, Z. J.; Wang, B.; Yan, J.; Li, J. J.; Cai, S. M. *Acta Chim. Sin.* **2001**, *59*, 1932–1936.

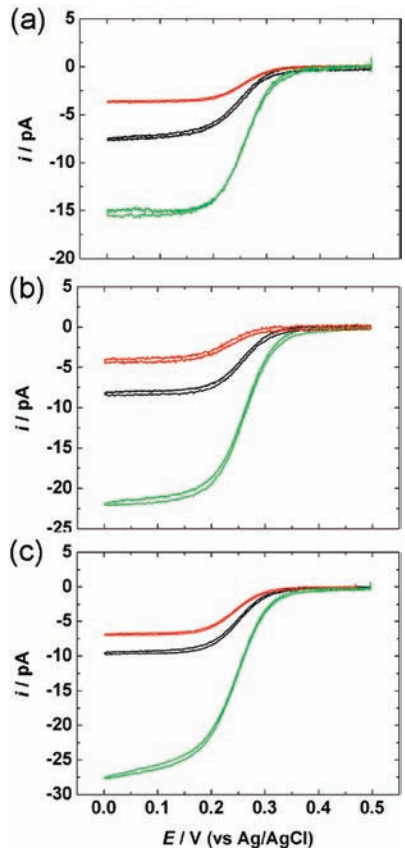

Figure 6. Voltammetric responses of 5.0 mM $K_3Fe(CN)_6$ in a 0.2 M KCl solution using bare Pt electrodes (black), APTMS-modified Pt electrodes (red), and Au SNPEs (green) (scan rate 10 mV/s). The diameters of the Pt electrodes and the Au SNPEs are about 8.0 and 14 nm (a), 9.0 and 18 nm (b), and 9.0 and 24 nm (c), respectively.

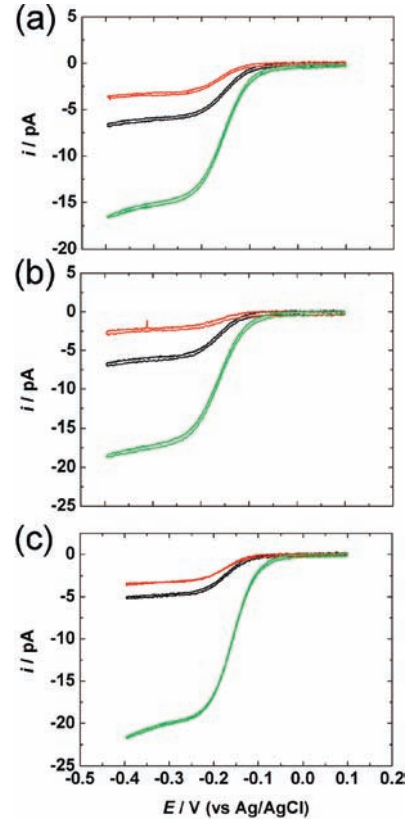

Figure 7. Voltammetric responses of 5.0 mM $Ru(NH_3)_6Cl_3$ in a 0.2 M KCl solution using bare Pt electrodes (black), APTMS-modified Pt electrodes (red), and Au SNPEs (green) (scan rate 10 mV/s). The diameters of the Pt electrodes and the Au SNPEs are about 7.5 and 14 nm (a), 6.8 and 18 nm (b), and 6.2 and 24 nm (c), respectively.

the 25 μm electrode, the silane modification results in around 80% inhibition of the limiting current from Figure 5. However, the inhibition is typically around 30−70% at nanoelectrodes as shown in Figures 6 and 7. We believe that the inhibition of the voltammetric current at the silane-modified electrodes is mainly due to an increase in the electron-transfer resistance caused by the increase in the electron-transfer distance, which is due to the presence of the silane SAM. The formation of high-quality silane SAMs is possibly easier at a microelectrode than at a nanoelectrode of less than 5 nm with more edge areas relative to the total surface at the nanoelectrode. Therefore, we believe the difference in the current inhibition at the microelectrode and the nanoelectrode is mainly due to more defects/edges in the SAMs at the Pt nanoelectrodes.

Another interesting aspect is that the voltammetric response on a silane-modified electrode shows a noticeable shift in $E_{1/2}$ relative to the bare Pt nanoelectrode, indicating that the voltammetric response is more irreversible at the silane-modified electrode than at the bare Pt electrode. For example, Figure SI2 (Supporting Information) gives a comparison of the normalized $i-V$ responses of Figure 6b. A ~30 mV potential shift can be seen from Figure SI2 for the APTMS-modified Pt electrode. However, $E_{1/2}$ of the $i-V$ response for the Au SNPE is approximately the same as that of the bare Pt, which indicates that the electron-transfer kinetics at the Au SNPE is rapid.

The steady-state current shown in Figure 6a has been significantly enhanced compared to that collected from the bare Pt nanoelectrode, which might be due to the larger size of the 14 nm Au nanoparticle relative to the disk Pt nanoelectrode (diameter 8 nm). Parts b and c of Figure 6 show similar responses at Au SNPEs prepared using 18 and 24 nm Au colloids, respectively. Similar steady-state voltammetric responses have also been observed using $Ru(NH_3)_6^{3+}$ as the redox species, as shown in Figure 7. The diffusion-limited steady-state current at the Au nanoparticle electrode is significantly greater than that at the Pt nanodisk electrode due to the larger size of the Au compared to the Pt.

The magnitude of the steady-state limiting current has been found to be determined by the size of the Au nanoparticle and to be less dependent on the size of the Pt nanoelectrode. The steady-state limiting current, i_d, at the Au nanoparticle electrode can be estimated using the following equation, assuming a spherical geometry at an infinitely large surface:[32]

$$i_d = 2\pi(\ln 2)nFDC_b a \quad (1)$$

where F is the Faraday constant, D and C_b are the diffusion coefficient and bulk concentration of the redox molecule, n is the number of electrons transferred per redox molecule, and a is the radius of the Au nanoparticle. The steady-state limiting currents at Au SNPEs have been obtained from the voltammetric responses in a 5 mM $Fe(CN)_6^{3-}$ solution, as listed in Table 1. Also listed in Table 1 are the values calculated using eq 1 on the basis of the average size of the Au nanoparticle observed from TEM characterizations, as shown in Figure SI1 (Supporting Information). At least five Au SNPEs have been utilized to obtain each voltammetric datum shown in Table 1. From Table 1, it can be seen that the steady-state limiting current at the Au SNPE measured from cyclic voltammograms (i_{cv}) is in fairly

Table 1. Comparison between the Measured and Calculated Steady-State Limiting Currents at Au SNPEs in 5 mM $Fe(CN)_6^{3-}$ [a]

	14 nm diameter Au	18 nm diameter Au	24 nm diameter Au
i_{cv} (pA)	13.5 ± 1.1	16.2 ± 2.8	22.4 ± 2.4
i_{calcd} (pA)	11.9 ± 2.7	15.3 ± 3.3	19.4 ± 2.8
difference (%)	13.4	5.9	15.4

[a] The measured values were obtained from steady-state voltammetry, and the calculated values were obtained from eq 1 on the basis of TEM characterizations.

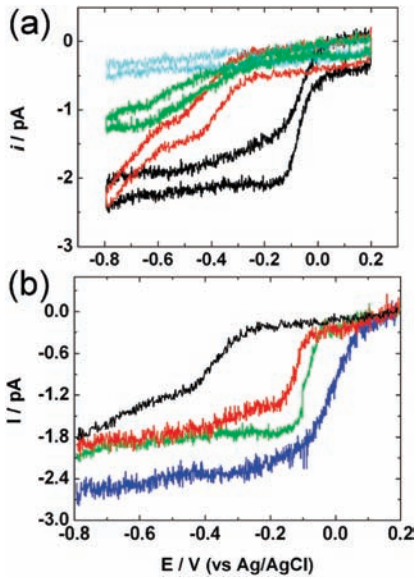

Figure 8. (a) Voltammetric responses of a 0.10 M KOH solution using an 18 nm Au SNPE (black), an APTMS-modified Pt nanoelectrode (green), the bare Pt nanoelectrode after oxygen is bubbled (red), and an 18 nm Au SNPE after nitrogen is bubbled (cyan). (b) Voltammetric responses of an oxygen-saturated 0.10 M KOH solution using a bare 7 nm diameter Pt nanoelectrode (black), a 14 nm Au SNPE (red), an 18 nm Au SNPE (green), and a 24 nm Au SNPE (blue). The scan rate was 10 mV/s.

good agreement with that estimated from TEM characterizations using eq 1 (i_{cal}) for the 14, 18, and 24 nm Au nanoparticles. The measured limiting currents are 13.4%, 5.9%, and 15.4% greater than those calculated from the 14 nm, 18 nm, and 24 nm nanoparticles, respectively. We are not entirely sure why the measured limiting current is greater than that estimated from the size of the nanoparticles. We speculate that the Pt electrode could possibly contribute to the measured faradic response. There are several possible methods to prevent the supporting nanoelectrode from contributing to the faradic responses. The first method is to decrease the size of the Pt nanoelectrode so that redox molecules will not be able to reach the supporting electrode due to hindrance from the nanoparticle. Second, longer silane linker molecules could be used to further decrease electron transfer between the Pt and the redox molecules. Alternatively, an inert electrode material could be used as the supporting electrode so that faradic processes can only happen at the nanoparticles.[31−33]

Oxygen Reduction at Single Au Nanoparticles. One of our goals in developing SNPEs is to study the structure−function relationship in nanoparticle-based electrocatalysis. To demonstrate that electrocatalytic responses can be obtained at a single-nanoparticle level, we have measured the voltammetric responses of the Au SNPEs in ORR. Figure 8a displays a comparison of the steady-state voltammetric responses in an oxygen-saturated aqueous solution containing 0.10 M KOH of the same Pt nanoelectrode before (red) and after (green) modification with APTMS and the corresponding 18 nm Au SNPE (black). The cyan curve in Figure 8a shows the voltammetric response of the Au SNPE in the same solution after degassing with a flow of N_2. In a 0.10 M O_2-saturated KOH solution, the bare Pt nanoelectrode exhibits a two-step process for oxygen reduction with onset potentials of ca. −0.35 and −1.0 V (not shown), respectively, indicating a two-step four-electron reduction pathway of O_2 to OH^- (through HO_2^- as an intermediate).[69−71] When a silane monolayer is attached at the Pt electrode, the half-wave potential for oxygen reduction is shifted to about −0.60 V and the limiting current is decreased significantly, which indicates that the ORR is significantly hindered by the silane monolayer. However, the Au SNPE exhibits a one-step process for the ORR with an increased limiting current than that obtained at the bare Pt nanoelectrode, and the process has a four-electron pathway.[18,69,72] Moreover, it can be seen that the half-wave potential for the ORR at the Au SNPE is shifted to −0.07 V compared to that of the bare Pt nanoelectrode. From the above results, it can be concluded that the Au SNPE has good electrocatalytic activity for the ORR.

Table 2. Electrocatalytic Activity for ORR Using Bare Pt Nanoelectrodes and Au SNPEs[a]

	bare Pt electrode	14 nm Au electrode	18 nm Au electrode	24 nm Au electrode
i_{lim} (pA)		1.0 ± 0.2	1.7 ± 0.4	2.0 ± 0.3
$E_{1/2}$ (mV)	−365 ± 25	−130 ± 17	−75 ± 10	−35 ± 7
i_{lim}/a (pA/nm)		0.14	0.19	0.17

[a] Pt electrode size ∼7.0 nm in diameter, CV scan rate 10 mV/s.

The electrocatalytic activity for the ORR has been compared at Au nanoparticles of different sizes. Figure 8b shows a comparison of the voltammetric responses in an oxygen-saturated aqueous solution containing 0.10 M KOH of a bare Pt nanoelectrode (black) and three Au SNPEs of different sizes (14 nm Au SNPE (red), 18 nm Au SNPE (green), and 24 nm SNPE (blue)). It can be seen that the steady-state limiting current increases with increasing size of the Au nanoparticle. The half-wave potentials at larger Au nanoparticles are also shifted to higher potentials, indicating higher catalytic activity at larger Au nanoparticles. A summary of the steady-state limiting current and the half-wave potential at three different Au SNPEs is given in Table 2. The average limiting currents have been found to be 1.0, 1.7, and 2.0 pA for the 14, 18, and 24 nm Au SNPEs, respectively. The half-wave potentials have been shifted from ∼−365 mV at the bare Pt nanoelectrode to −130 mV at the 14 nm SNPEs, −75 mV at the 18 nm SNPEs, and −35 mV at the 24 nm SNPEs.

The peak current has been utilized to compare the electrocatalytic activity of nanoparticle arrays at macroscopic electrodes. However, unlike macroelectrodes for which the peak current is proportional to the surface area,[73] the limiting current is proportional to the radius of the electrode for a spherical nanoelectrode. Therefore, the steady-state limiting current should

(69) El-Deab, M. S.; Sotomura, T.; Ohsaka, T. *Electrochem. Commun.* **2005**, *7*, 29–34.
(70) Pletcher, D.; Sotiropoulos, S. *J. Chem. Soc., Faraday Trans.* **1995**, *91*, 457–462.
(71) Birkin, P. R.; Elliott, J. M.; Watson, Y. E. *Chem. Commun.* **2000**, 1693–1694.
(72) El-Deab, M. S.; Ohsaka, T. *Electrochem. Commun.* **2002**, *4*, 288–292.
(73) Bard, A. J.; Faulkner, L. R. *Electrochemical Methods*; John Wiley & Sons: New York, 2001.

be normalized to the radius of the Au nanoparticle to estimate the electrocatalytic activity for ORR, and the results are also listed in Table 2. It can be seen that the normalized steady-state limiting currents are 0.14, 0.19, and 0.17 pA/nm for the 14, 18, and 24 nm Au nanoparticles, respectively. The 18 nm Au nanoparticles show slightly better electrocatalytic activity for ORR than the 14 and 24 nm particles. The half-wave potentials for ORR at the Au nanoparticles are significantly higher than that at the bare Pt nanodisks, indicating higher electrocatalytic activity at the Au nanoparticles than at the Pt disks. Further investigation of the half-wave potentials from Table 2 indicates that the 24 nm Au nanoparticles possibly have higher catalytic activity than the smaller nanoparticles due to a slightly higher half-wave potential toward ORR. Further experiments are needed to quantitatively understand how the voltammetric responses of the Au nanoparticles could depend on the size and the material of the nanodisk and the properties of the linker molecules. These experiments are ongoing in our laboratory.

Conclusions

We have demonstrated the construction and characterization of the Au SNPE. The Au SNPE has been characterized by means of TEM, steady-state voltammetry, and UPD. It has been shown that the presence of a single Au nanoparticle can greatly enhance the electron transfer from the Pt to the redox molecules. The voltammetric response at Au SNPE depends more on the size of the Au nanoparticle than the size of the Pt nanoelectrode. The Au SNPE has been utilized to examine the ORR in a KOH solution to explore the feasibility of comparing electrocatalytic activity at a single-nanoparticle level. It has been found that Au SNPEs exhibit good size-dependent electrocatalytic activity toward ORR, which could also be affected by the Pt nanoelectrodes.

Acknowledgment. We gratefully acknowledge financial support from the University of Washington. TEM imaging was performed by Dr. Xiaoxia Gao at the UW Nanotech Center. Part of this work was conducted at the University of Washington NanoTech User Facility, a member of the NSF National Nanotechnology Infrastructure Network (NNIN). We thank Prof. Daniel A. Buttry for suggesting the Cu UPD experiments.

Supporting Information Available: Fabrication of the Pt microdisk electrode, TEM images of Au nanoparticles, and more voltammetric responses of Au SNPEs in $K_3Fe(CN)_6$ and $Ru(NH_3)_6Cl_3$. This material is available free of charge via the Internet at http://pubs.acs.org.

JA909408Q